SkinTrack: Using the Body as an Electrical Waveguide for Continuous Finger Tracking on the Skin

Yang Zhang[1]   Junhan Zhou[2]   Gierad Laput[1]   Chris Harrison[1]

[1]Human-Computer Interaction Institute, [2]Electrical and Computer Engineering Department

Carnegie Mellon University

5000 Forbes Avenue, Pittsburgh, PA 15213

{yang.zhang, gierad.laput, chris.harrison}@cs.cmu.edu, junhanz@ece.cmu.edu

ABSTRACT

SkinTrack is a wearable system that enables continuous touch tracking on the skin. It consists of a ring, which emits a continuous high frequency AC signal, and a sensing wristband with multiple electrodes. Due to the phase delay inherent in a high-frequency AC signal propagating through the body, a phase difference can be observed between pairs of electrodes. SkinTrack measures these phase differences to compute a 2D finger touch coordinate. Our approach can segment touch events at 99% accuracy, and resolve the 2D location of touches with a mean error of 7.6mm. As our approach is compact, non-invasive, low-cost and low-powered, we envision the technology being integrated into future smartwatches, supporting rich touch interactions beyond the confines of the small touchscreen.

Author Keywords

Finger tracking; waveguide; smartwatch; on-body interaction; around-device interaction; ADI

ACM Classification Keywords

H.5.2. [User interfaces] – Input devices and strategies.

INTRODUCTION

Small wearable devices—such as smartwatches and digital jewelry—are fast becoming viable computing platforms. However, their small size severely limits the user experience. For example, touchscreens on smartwatches suffer not only from a paucity of interactive surface area, but also must contend with significant finger occlusion. In general, the interfaces on these devices rely on basic input modalities (often four or fewer onscreen buttons, or even just directional swipes). In response, many research efforts have investigated how to leverage the area *around* devices to open new and potentially larger input modalities.
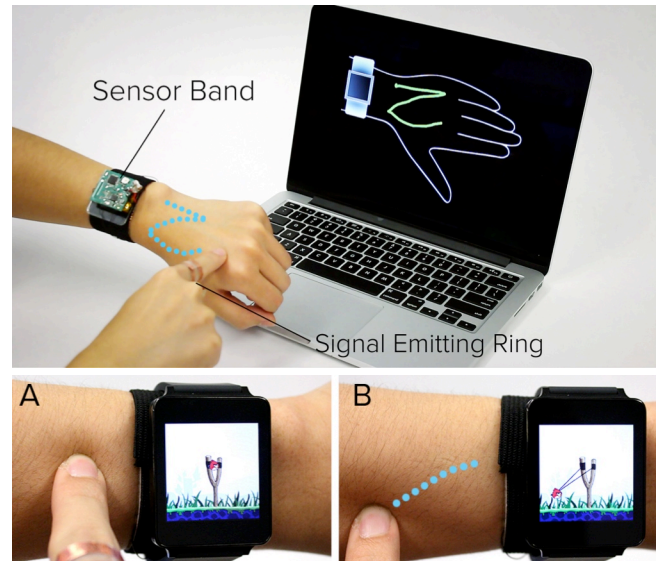
Figure 1. Our sensor band and signal-emitting ring allow the arm to be appropriated for continuous, on-skin touch tracking (top), expanding interaction beyond the small confines of a smartwatch touchscreen (bottom).

In this paper, we propose a novel sensing approach for appropriating the skin as an interactive, touch-tracking surface (Figure 1). Our system, *SkinTrack*, has two key components. First is a ring that emits an imperceptible and harmless 80MHz, 1.2Vpp AC signal into the finger on which it is worn. The second component is a wristband, worn on the opposite arm, and instrumented with a structured electrode pattern. When the user's finger touches the skin, the electrical signal propagates into the arm tissue and radiates outwards. As we will discuss in greater detail later, the signal takes time to propagate, which means electrodes located at different places around the wrist will observe characteristic phase shifts. By measuring these phase differences across several electrode pairs, SkinTrack can compute the location of the signal source (i.e., the finger), enabling real-time touch tracking on the skin.

Compared to prior work, our approach requires no direct instrumentation of the touch area (i.e., a skin overlay) or sensor line-of-sight (i.e., cameras). It also has a high signal-

to-noise ratio (SNR), is unaffected by lighting conditions, and even works through clothing. Results from our user study demonstrate high reliability and accuracy with a mean distance error of 7.6mm. We also ran several supplemental and targeted experiments to further quantify performance and feasibility, which reveal similar promising results. Finally, we built a series of example applications to demonstrate the interaction modalities supported by SkinTrack.

RELATED WORK
SkinTrack intersects with several broad research areas; we briefly summarize key related work.

Appropriating the Skin as an Input Surface
The skin offers an always-available, tactile surface on which to perform interactions. A wide variety of technical approaches have been explored. Most straightforward are worn overlays, which directly augment the skin's surface with thin, soft, and deformable materials equipped with sensing capabilities [26,28,50]. For example, iSkin [53] uses a bio-compatible, stretchable "sticker" impregnated with conductive traces, which can capacitively sense finger touches. Likewise, interactive textiles [43] function as transient overlays. Finally, it is also possible to more permanently implant sensors under the skin [23].

It is often desirable to avoid directly instrumenting the input area and instead sense touches with remote sensing. For example, sound, like electricity, can conduct through the body, which has led to the development of several bio-acoustic sensing systems [19,36]. It is also possible to use, e.g., range-finding sonar directly above the skin surface for finger tracking [33]. Likewise, electrical signatures measured on the bare skin can be leveraged to detect which part of the human body is being touched [35]. Using a fingerprint sensor, SkInteract [41] detects discrete locations and orientations on a user's hand. Optical approaches are also popular, the simplest of which use infrared proximity sensors [31,37,40]; more sophisticated are systems that use depth sensors and cameras to track finger contacts [10,20].

SkinTrack improves upon previous approaches in several ways. For example, Skinput [19] can only detect touches on discrete pre-learned skin locations. Mujibiya et al. [36] extends this sensing capability to enable continuous touch sensing, but their approach can only sense 1D discrete gestures (i.e., swipes). In comparison, SkinTrack computes a finger's position on the skin in continuous 2D space. Further, SkinTrack can be worn on the wrist (like a smartwatch) with the signal-emitting ring worn normally, whereas the aforementioned systems uses a forearm placement. Further, although OmniTouch [20] supports fully continuous 2D touch tracking, the shoulder-mounted depth camera is socially obtrusive. Finally, as we will show later, SkinTrack can also track a finger hovering above the skin, a capability offered by few on-body systems.

Expanding Smartwatch Interaction
Researchers have also investigated smartwatch input techniques that extend beyond the standard touchscreen.

For example, WatchIt [52] proposed using the watchband for touch input (e.g., as a slider), NanoTouch [3] moved the touchpad to the rear of the device, while Ashbrook et al. [1] utilized the watchface bezel. Likewise, Xiao et al. [56] use the watchface for coarse physical manipulations, such as twisting and tilting. Non-touch interactions are also possible, for instance, above- and around-device finger and hand tracking have been demonstrated with magnetic tracking [6,18]. Infrared proximity sensing has also been used, as seen in Ni et al. [38], Gesture Watch [29], and HoverFlow [30]. Lastly, Tomo [58] measured cross-sectional impedance of a user's wrist to detect muscle movement, enabling smartwatch control with hand gestures.

Ring Form Factors
Significant advances in the miniaturization of electronics have enabled "smart rings" to be developed, and used for both output (see e.g., [45]) and input purposes. For example, LightRing [27] uses an infrared proximity sensor and gyroscope to track finger movement and clicks, much like a mouse. eRing [54] uses an electric field to detect finger posture and dynamic finger gestures. Others have explored finger-worn cameras; for example, Yang et al. [57] tracks finger translation and can recognize properties of the touched surface, while SmartFinger [42] can recognize devices or touched content, such as telephone numbers. Similarly, CyclopsRing [4] uses a fisheye lens to enable whole hand and context-aware interactions. By correlating accelerometer data from different devices and objects, PickRing [55] can infer picked up objects; TypingRing [39] enables text entry on an ad-hoc surface. Finally, Abracadabra [18] and Nenya [2] both employ rings with permanent magnets, which can be tracked by a magnetometer operating in a proximate smartwatch.

Using the Human Body as an Electrical Conduit
The human body is conductive, which means it can function as a conduit for sending and receiving electrical signals. This property been used extensively for personal area networks (PANs), which modulate an electrical signal onto the skin [14] for digital communication purposes. Other systems have used this property for human-computer input. For example, DiamondTouch [11], an early multi-user interactive whiteboard, used different ground paths to differentiate touches from several users. Touché [49] detects configurations between objects and the human body by generating a swept frequency signal and analyzing the impedance curve response. By using though-body electrical signals, Capacitive Fingerprinting [21] and Biometric Touch Sensing [24] can differentiate between users. Passive techniques are also possible, such as Humantenna [7,8] and EM-Sense [32], which monitor electromagnetic noise absorbed by the human body for e.g., gesture and object recognition.

SKINTRACK SENSING PRINCIPLE
SkinTrack relies on the principles that govern electromagnetic (EM) waves propagating along a physical waveguide. As the human body is conductive, the arm can operate as a
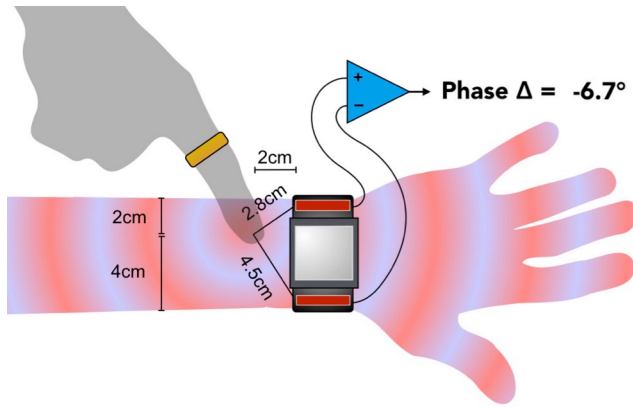
Figure 2. A finger's location on the skin will produce varying phase differences observed by electrode pairs. Note the waveform "ripple" is illustrative and not drawn to scale.
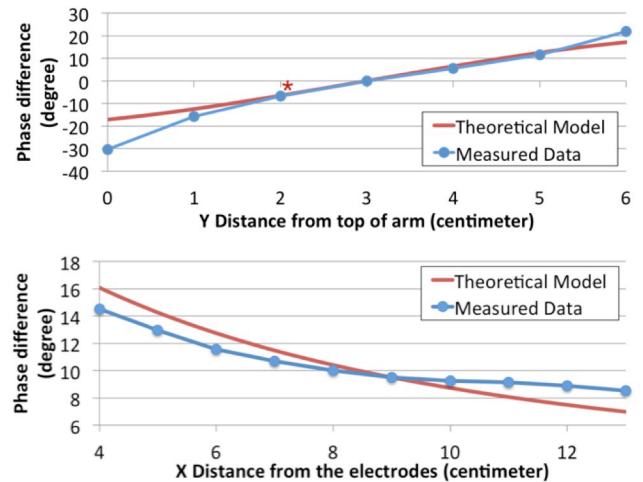

Figure 3. Phase differences computed from theoretical models vs. collected data using SkinTrack. The asterisk in the upper figure matches the geometry illustrated in Figure 2.

waveguide [25] for electrical signals [13,16,34,46]. In the human body, the skin has an average permittivity of 17 at 80MHz [15], which means an 80MHz electromagnetic wave propagates at 7.3×10^7 m/s, with a peak-to-peak wave length of ~91cm. Our ring emits an 80MHz AC signal, which results in a phase difference of ~4° per cm traveled.

Figure 2 offers a simple schematic example. Here, a finger wearing our signal-emitting ring is touching the skin 2cm to the left of the smartwatch and 1cm above the midline of the arm. The smartwatch has two skin-bound electrodes (in red) separated by 6cm. In this example, the finger is 2.8cm and 4.5cm away from the two electrodes—a *difference* of 1.7cm. This results in a phase difference of 6.7° (using an 80MHz signal), which can be determined by a phase comparator (blue triangle). This electrode arrangement is most sensitive to movement along the y-axis (we employ different electrode arrangements to best capture x-axis translations).

To verify our model, we manually measured the phase difference at known locations on the skin and plotted these against expected values derived from our model. Specifically, we drew seven crosshairs in a vertical arrangement (offset 2cm from the left of the smartwatch) at 1cm intervals. As can be seen in Figure 3 (top), these results largely match what we predicted. We also marked the arm with ten crosshairs running horizontally along the arm (offset 4cm to the left of the smartwatch) at 1cm intervals. We used a different electrode pair (perpendicular to that in Figure 2) to capture x-axis movements. As before, the measured phase differences track remarkably well with what our model predicts (Figure 3, bottom). We suspect these small differences are likely due to arm curvature, variations in tissue composition, and also the fact that the electrodes are not discrete points on the skin, but rather small patches – none of which are controlled for in our model.

IMPLEMENTATION

As noted earlier, SkinTrack has two hardware components: a signal-emitting ring and a sensor band. We now describe how these were implemented, along with our system's signal processing and machine learning components.

Signal Emitting Ring

Our ring's chief component is an oscillator driven by a 3.3V voltage regulator. This generates an 80Mhz sine wave at 1.2Vpp. This ring consumes 7mA when operating. Thus, for a 110mAh LiPo battery (2×1×0.5cm), we can continuously power the ring for roughly 15 hours. Experiments revealed that higher signal amplitudes result in superior SNR, but at the cost of increased power consumption.

The oscillators signal pin and the ground pin are connected to parallel electrodes wrapping around the finger (Figure 4). The two strips of copper have a current flow longitudinal to the finger, an arrangement that generates optimal SNR with minimal energy radiating into free air (per prior work, e.g., [13,46]). This also allows the system to be more sensitive to true physical finger touches (and not just proximity of the fingers). Finally, a thin layer of Mylar was used to cover the electrodes to ensure that only capacitive coupling exists between the finger and the electrodes. The Mylar layer obstructs DC current, which not only reduces power consumption from 12 to 7mA (without resolution loss), but it also mitigates signal variations from e.g., sweat and inconsistent skin coupling.

We performed multiple experiments to select the most appropriate frequency for the ring's active oscillating signal. There were three key considerations. First, the frequency must be high enough to ensure that propagation delays induce measurable phase differences between any two fixed points. If the frequency is too low, the phase difference will be too small to measure accurately; if the frequency is too high, the wave could complete a full cycle during propagation, producing ambiguous positions due to wraparound. Second, oscillator power consumption generally increases with higher frequencies (when output voltage is held constant). Thus, the frequency should be chosen as low as permissible to save power. Finally, signals with
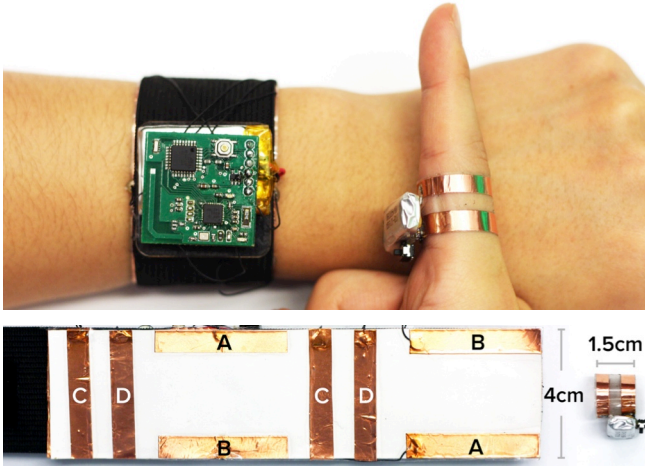
Figure 4. Sensor band and signal-emitting ring (top).
Electrode layout and dimensions (bottom).

higher frequencies more readily radiate into open air [16,34], which can cause interference and multipath issues. The ideal signal should be sufficient low in frequency such that the signals chiefly propagate though the human body.

We experimented with a wide range of frequencies during development (from 5MHz to 600MHz) and found 80MHz to be best when weighing these different considerations. An 80MHz signal has a wavelength of 91cm on the skin, which is roughly twice the length of the average forearm (i.e., no phase wraparound possible). Further, testing revealed that 80MHz doesn't freely radiate into the air, and oscillators operating at this frequency have relatively lower power consumption.

Sensor Band
Our wristband uses Analog Devices' AD8302 RF/IF gain and phase comparator chips [9]. Each AD8302 takes two signals as input, and computes the gain and phase differences (output as analog values). It provides an accurate measurement of gain ratio over a ± 30dB range scaled to 30mV/dB, and of phase over a 0°–180° range scaled to 10 mV/°. To improve SNR, we replaced the input termination resistors from the recommended 52.3Ω to 50MΩ. Further, we placed capacitors between the resistors and electrodes to form a high pass filter, dampening low frequency environmental EM noise (e.g., 60Hz power line). This setup captures a receiving signal of around 23mVpp when the signal-emitting finger is touching the skin.

We used four phase comparator chipsets to measure signals captured by our four pairs of electrodes (Figures 4 and 5). Letters denote electrode pairings in Figure 4. Pair 'A' and 'B' were tuned to be sensitive to movements along the x-axis, and 'C' and 'D' for y-axis. Since the AD8302 can only detect absolute phase differences (i.e., no absolute reference point), we strategically positioned the eight electrodes around the wristband to get the most distinguishable phase differences. We used a ground plane parallel to the skin to shield these electrodes and further increase the
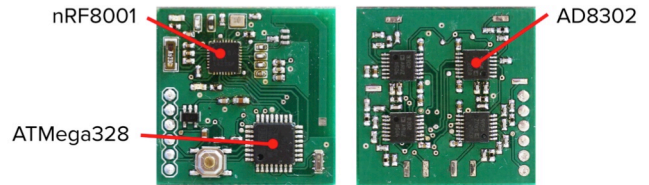

Figure 5. SkinTrack prototype circuit board (front and back).

SNR. Note that the four pairs of electrodes are symmetric in all directions, allowing our system to sense all four input locations (discussed later) without rotating the band. Similar to our ring's construction, we used a thin Mylar layer between the electrodes and the skin to ensure a robust capacitive coupling.

In total, our prototype sensing board (Figure 5) produces eight analog values — one phase difference and one gain ratio for each of the four comparison channels. These outputs are sampled using an ATMega328 microcontroller running at 8MHz, which has eight 10-bit analog-digital converter (ADC) channels. A *Nordic* NRF8001 Bluetooth Low Energy (BLE) chip transmits these values at approximately 30 updates per second. We found this frame rate to be fast enough to support interactive touch tracking. Superior frame rates are possible with a faster ADC and higher-throughput wireless communication (moot if integrated into a smartwatch).

Machine Learning
Our machine learning pipeline for touch tracking has two stages: First we *classify* whether the skin is being touched, and then we track the touch points using *regression* models. Our implementation utilized the Weka toolkit [17]. Once trained, our classifiers are easily computed in real-time on embedded processors.

Feature set
We used the four gain ratios and four phase differences in our feature set, as they were inherently discriminative. We also included the differences between all pairs of the eight data points (without repetition), resulting in 28 additional features. Further, we computed the mean, median, max, min, range, standard deviation, and sum within the group of gain ratios and group of phase differences respectively, providing 14 additional features. In total, this yielded 50 features. Both our touch classifier and finger position regression models utilized this feature set.

Touch Classification
We used a first-level classifier to detect whether the skin was being touched. For this, we used a support vector machine (SVM) classifier with default parameters (RBF kernel, $\gamma=0.3$). If a touch was detected, it triggered additional computation for finger tracking, described next.

Finger Position Regression
Once a touch was detected, we used regression models to compute the finger's 2D skin coordinate. We used two, independent regression models (SMOReg, RBF kernel,

γ=0.7), which operated in parallel – one for X position and another for Y position. To train the regression models, we marked 3×3 crosshair matrices on the user's skin with a 30mm interval between crosshairs (Figure 6).

EVALUATION

We designed a series of user studies to answer two paramount questions: 1) how accurately can SkinTrack segment touch events on the skin, and 2) how accurately can SkinTrack localize these inputs on the skin. In response, we recruited 12 participants (3 female, mean age=26). Since all participants were right handed, they wore the sensing band on the left wrist (the traditional location to wear a watch). The ring was worn on the index finger of the right hand (see Figure 4, top).

To summarize, we collected three rounds of training data, followed by three rounds of live testing. Following a short break, three more rounds of live testing were conducted. The study lasted around 1 hour; participants were paid $10.

Setup

We first collected basic user demographic and biometric information, including gender, age, wrist radius, elbow radius, arm length, height, weight, and arm hairiness. We then affixed our sensor band and ring to the participant.

A smartwatch naturally segments the arm into four input locations: the *front* and *back* of the *hand*, and the *front* and *back* of the *forearm* (see Figure 6). For each of these location conditions, we drew a 3×3 crosshair patterns (with a 30mm interval) on participants' skin with a washable marker. For the two *hand* locations, the crosshair matrix was centered in the area between the wrist and base of the fingers (e.g., middle of the palm). For the two *forearm* conditions, the matrix was centered between the left edge of the smartwatch and the elbow joint.

The four input locations were trained and tested sequentially and in a random order. For each input location (front arm, back hand, etc.), we trained and tested as follows:

Training

First, participants were asked to keep their finger approximately ten or more centimeters above the arm, and move back and forth in a roughly "W" shape. Over a 10 second period, 270 data points were collected and recoded as finger "*out of range*" instances. The laptop emitted a beep when collection was complete. Next, a laptop display highlighted one of the nine possible crosshairs. Participants moved their finger to this location, and held their finger approximately 1cm above the skin. Over a 1 second period, 30 data points were captured and saved as "*hover*" instances, followed by a beep. Then, for the same crosshair location, the user touched the skin with their finger. Over a 2 second period, 60 data points were captured and saved as "*touch*" instances. As before, the laptop emitted a beep when complete. Each crosshair appeared exactly once and in random order.

This procedure constituted one round of training data collection. This was repeated twice more, for a total of three

training data rounds. To train our click detection classifier, we combined *out of range* and *hover* instances into a unified *no touch* class (1620 instances), which was paired with the 1620 *touch* instances. We used all *touch* instances to train our X/Y regression models.

Testing

For the most realistic results, we tested SkinTrack *live* (i.e., no post hoc calibrations or algorithm tweaks). The order of the testing procedure was the same as the training procedure: First, 270 *out of range* examples were evaluated over 10 seconds, followed by 30 *hover* and 30 *touch* examples for each of the nine crosshair locations. However, unlike before, the system performed real-time classification of touch state and finger X/Y location, which was also saved for later statistical analyses. This testing procedure was repeated two more times, for a total of three testing rounds, resulting in 810 *out of range* instances, 810 *hover* instances, and 810 *touch* instances. This process was repeated for the four input locations (random order). In total, this meant our 12 participants produced 116,640 test instances.

We then asked participants to remove the sensor band and rest/stretch their arms/hands, as well as walk around the lab space. After a few minutes, the sensor band was re-affixed to the wrist in roughly the same position, though no special controls or alignment were used (other than what the user deemed to feel natural). This was followed by a second block of testing using the same procedure as above. This data was used for the subsequent "Stability Following Band Removal" analysis.

Of note, during testing, participants were given no feedback (verbal, graphical or otherwise) to prevent them from adjusting e.g., their touch position to adapt to classification/regression results.

RESULTS

We now describe the results of our evaluation, along with several ancillary results that help quantify other aspects of our system's performance and reliability.

Touch Detection Classification

Across 116,640 trials, our system achieved 99.0% *touching* vs. *not touching* classification accuracy. There were no significant differences between our four input location conditions: *Back Hand* achieved 98.4% (SD=1.8%), *Front Hand* 99.6% (SD=0.7%), *Back Arm* 98.9% (SD=1.0%), and *Front Arm* 99.1% (SD=0.9%).

As noted previously, *not touching* was the union of two sub-classes: *out of range* and *hover*. When keeping these classes separate, and also including *touch* as a finger state (i.e., a three-class classifier), mean live accuracy across the four input locations was 98.5% (SD=3.5%), essentially the same as *touching* vs. *not touching* accuracy.

Finger Tracking Spatial Accuracy

We used the data from the first block of testing to assess the spatial accuracy of finger tracking. In testing, for each crosshair touch trial, 30 position estimates were collected

30mm

Back Arm   Back Hand (Palm Down)   Front Arm   Front Hand (Palm Up)
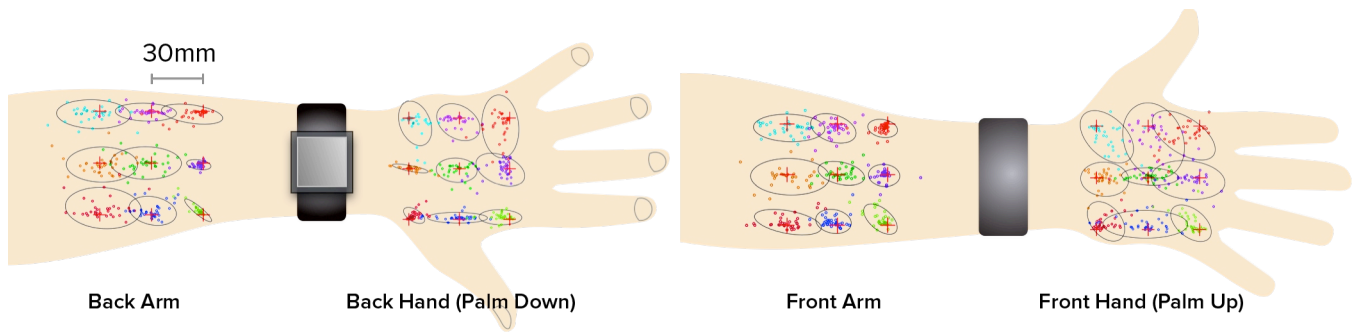
Figure 6. Our four input locations and all-participant click distributions. 2σ confidence ellipses capture 97.8% of touches.

sequentially over a one second period. We use all 30 positions for a post hoc analysis described later, but used only the very first position estimate for this live assessment. Although this precluded any ability to smooth or filter the estimated touch position, it also ensured the lowest input latency (~33ms).

Combining data from all crosshairs and input locations, mean positional error is 7.6mm (SD=1.2mm). This result compares favorably to other on-body finger tracking systems (see e.g., [19,20,33]). We found no significant difference between input locations.

Another way to visualize this result is to compute how large targets would have to be (i.e., buttons) in order achieve a specified "click" accuracy. This analysis was performed in OmniTouch [20], and we followed the procedure outlined in the paper. Specifically, we first removed outlier touch trials – those lying greater than three standard deviations away from the mean absolute difference between the recorded touch point and the intended crosshair (28 trials, 2.2% of our data). We then plotted confidence ellipsoids encompassing 97.8% (i.e., mean + 2σ) of touches for each crosshair, across all four input locations.

This result, drawn to scale, is illustrated in Figure 6. In general, accuracy reduces the farther touches are away from the sensor band. This is because the relative Euclidean distance delta between electrodes pairs decreases, along with SNR. Figure 7 offers a direct comparison to OmniTouch [20] (blue) and also plots a result found by Holz et al. [22] for conventional capacitive touchscreens (orange).

Latency vs. Accuracy Tradeoff
In our "Finger Tracking Spatial Accuracy" results section, we used the very first position estimate reported by Skin-Track to achieve minimum input latency. However, it is often advantageous for sensors to sample several data points and combine them (e.g., mean) to achieve a superior resolution. To investigate this, we configured our experiment code to record 30 position estimates sequentially over a one second period for each crosshair trial.

We then used this data to compute the mean of an ever-enlarging pool of positional readings. In other words, at t=1, only the first sensed location is used. At t=10, the average consists of the first ten readings, and so on, up to all 30 data points being used (i.e., around one second of data collection at current sensor frame rate). We found that although positional accuracy increases as more sensor readings are integrated into the average, the gain is modest—an improvement of only 0.1mm—and likely not worth the cost of the increased latency (Figure 8).

Stability Following Band Removal
The previous section looked at performance when Skin-Track was trained and tested on a user without removal. Indeed, this is how most on-body systems are tested, as they are typically very sensitive to body placement (e.g., bio-acoustics [19,36], EMG [47,48], and capacitive sensing [44,58]). However, it is unrealistic to expect users to never remove a device. Thus, we wished to better understand the accuracy reduction that occurs when SkinTrack is removed and replaced on the skin, *without recalibration*.
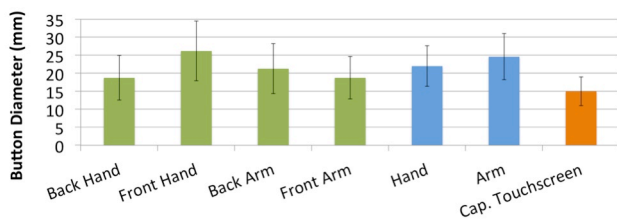

Figure 7. The button diameters (mm) necessary to encompass 97.8% of touches (2σ). Comparative results from OmniTouch [20] are shown in blue; Holz et al. [22] in orange. Error bars represent standard deviation across users.
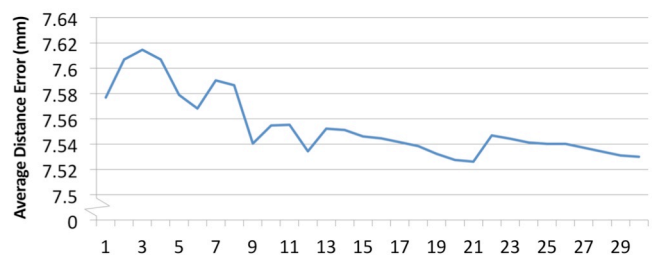

Figure 8. Average distance error over time. X-axis represents number of sensor readings utilized in the average (30 updates per second, up to one second).
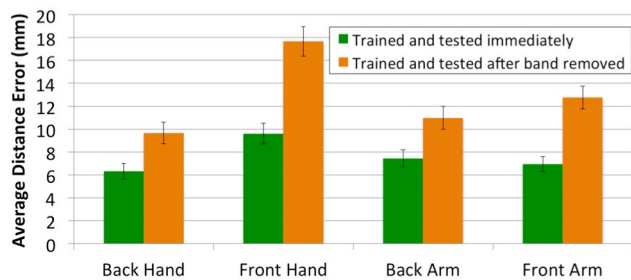
Figure 9. Average distance error (with standard error).

As described in our study procedure, we conducted a second block of testing that followed a brief break where the sensor band was removed. Once the sensor band was re-worn, we found that *touching* vs. *not touching* classification accuracy decreased to 96.8% (SD=0.65%), a 2.2% reduction, though this result is not statistically significant. The average positional error was 12.8mm (SD=3.0mm), an increase of 5.2mm (Figure 9), which is significantly worse that pre-removal accuracy (p<.05). This result suggests that SkinTrack, like most other bio-sensing systems, is similarly sensitive to sensor replacement.

Hover Sensing Spatial Accuracy
Although not a focus of the study, our experimental design naturally produced *hover* trials associated with an X/Y position (where users hovered above a target crosshair, before descending to touch it). Thus, it was easy to integrate a real-time validation of hover tracking accuracy. More specifically, we used hover data collected during the three training rounds to create regression models (SMOreg, RBF kernel, γ=0.1) for the X- and Y-axes. These ran in parallel with the X/Y touch regression models.

Because of the air gap between the finger and skin, less signal is transmitted into the arm. However, at these high frequencies, there is still some transmission, with the arm acting like an antenna. However, this is lossy and the signal is attenuated, reflected and otherwise distorted. Nonetheless, we found that basic tracking is still possible (see Video Figure), though at reduced spatial precision: a mean distance error of 12.0mm (SD=8.6mm) for *Front Arm*, 11.8mm (SD=9.7mm) for *Back Arm*, 12.7mm (SD=8.8mm) for *Front Hand*, and 7.6 mm (SD=6.3mm) for *Back Hand*.

Though offering reduced finger tracking resolution, we take advantage of this hover capability in one of our example applications (*Buttons and Keys*, Figure 12), as prior research has demonstrated the utility of combing hover and touch interactions [5].

Input Location Sensing
Given that we collected data across four input locations, we were curious if a classifier could be built that could discern which location was being touched, as thus be used to load the appropriate X/Y regressions for that particular body location. To explore this, we conducted a post hoc experiment using data collected during our live testing.

For a single participant, we used all *touch* trials from a single location (all three rounds from training block one), and relabeled them as one of the four possible classes: *Back Arm*, *Front Arm*, *Back Hand* and *Front Hand*. This was used to train a four-class SMO classifier (RBF kernel, γ=0.3). We then evaluated this model using the first block of testing data, revealing a location-sensing accuracy of 97.0% (SD=3.7%).

Cross-User Accuracy
An ideal sensing technique is accurate even when it has never seen a user before (i.e., no per-user training or calibration). This is particularly challenging for on-body sensing methods, as bodies vary substantially across people.

To test SkinTrack's ability to scale across users with a *general-purpose classifier*, we used our collected data to run a post-hoc simulation. Specifically, we trained our classifiers and regression models using training data from eleven participants, and tested on a twelfth's data (all combinations). We found that touch/no-touch classification accuracy dropped to 92.6% (SD=3.7%) across all participants and input positions. Similarly, the mean distance error of finger tracking increased to 24.1mm (SD=3.3mm). This suggests that although some common signal is present to enable coarse tracking, more research is required to help close this gap and achieve more practical accuracies.

Demographics and Biometrics
An F-test showed no significant effect for any of the demographic or biometric factors we collected, including gender, age, wrist radius, elbow radius, arm length, body-mass index (BMI), and arm hairiness. One biometric had borderline significance—hairiness (p=.052). For this, we used an informal three-point scale based on hair thickness observed on participants' forearms. We found a slight trend of reduced touch spatial accuracy as hair level increased: "none or light hair" had a mean distance error of 6.9mm (SD=3.1mm), while "medium hair" and "dense or long hair" showed means of 11.3mm (SD=6.8mm) and 11.8 (SD=6.2) respectively. However, we caution that our participant pool is small, and thus it is hard to make robust conclusions.

SUPPLEMENTARY EVALUATION
Following our main user study, we conducted several smaller and more focused supplemental studies. For these experiments, we recruited three new participants (all male, with a mean age of 25). The experimental setup was the same as the main user study.

High Spatial Resolution and Sensing Distance
In order to keep our main user study under one hour in duration, it was necessary to use crosshair grids only 3×3 in size. Unfortunately, this lacked spatial variety on which to properly train a regression model, though even with limited training data, our models were still sub-centimeter accurate.

Thus, in this supplemental experiment, we doubled the density of our crosshair grid (15mm intervals, instead of
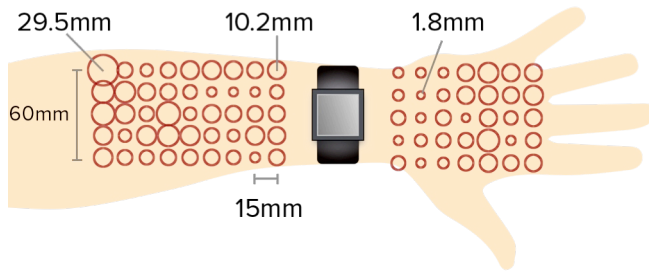
Figure 10. Distribution of finger tracking error on the back of the arm when the X/Y touch regressions are trained on higher resolution data. Diameters represent mean distance error for each crosshair and are drawn to scale.

30mm previously), and also extended the input area. Specifically, we used a 9×5 grid for *Back Arm* and a 7×5 grid for *Back Hand* (Figure 10). We did not evaluate either front input locations, but the results should be similar. We used the same data collection procedure as the main study, but only collected one training and one testing round, due to the large number of crosshairs (80 in total). The result, drawn to scale, is shown in Figure 10; mean distance error was 8.9mm (SD=4.7mm). As before, error increases as the finger moves farther away from the sensor band.

Discrete Finger Sensing
As previously demonstrated by several on-body systems [19,48], the discrete nature of fingers makes them ideal "buttons" for e.g., triggering different interactive functions. Thus, we tested if SkinTrack could recognize touches to each of the five fingertips. Specifically, we defined six class labels: *no touch*, *thumb*, *index*, *middle*, *ring* and *little* fingers. From each of our three participants, and for each class, we collected 90 data points (3 rounds of 30 data points). We used this training data to initialize a six-class SMO classifier (Polynomial kernel, E=1.0), which uses the same feature set as previous sections. We then tested finger classification accuracy live, which yielded 91.8% accuracy (SD=7.7%).

Clothing
Clothing can significantly disrupt on-body sensing systems, especially those employing optical approaches (e.g., IR proximity, cameras). Thus, we were curious how well our approach would function if a layer of clothing was introduced *post-training*. We had our three participants wear long sleeve shirts (roughly 1mm in thickness), initially rolled up behind the elbow. Matching our main user study, we collected three rounds of training data on a 3×3 crosshair grid for the *Back Arm* location.

We then immediately moved to live testing (also using the same procedure as our main study), yielding a mean distance error of 10.0mm (SD=6.7mm) with the sleeves up. We then pulled the sleeves down, covering the target crosshairs, and repeated the live accuracy testing (i.e., no retraining). Encouragingly, we found no degradation in tracking accuracy (9.7mm sleeves down vs. 10.0mm mean error sleeves up). However, touch/no-touch classification accuracy dropped slightly to 97.8% (vs. 99.3% sleeves up). This suggests that despite adding an insulating layer, the signal can readily propagate through at least thin clothing.

Skin Moisture
The electrical properties of the skin can vary based on moisture level (e.g., perspiration or washing of the hands). To investigate if this affected SkinTrack, we had our three participants train the system (same procedure as above), followed by immediate live accuracy testing. Participants then wiped their arm with a wet paper towel to moisten the skin at a level similar to having just washed ones' hands. Using the same classifier, we ran a second round of live testing. Mean distance error for pre- and post-moisturization was 10.0mm (SD=6.7mm) and 9.4mm (SD=6.1mm) respectively; touch/no-touch classification appeared similarly unaffected (97.9% vs. 97.5%).

Ring on a Different Finger
For all previous experiments, the signal-emitting ring was worn on the index finger, which was also used for input. Although the index finger is often used for touch interaction, it is more typical for rings to be worn on the ring finger. In response, we ran one final supplemental study that had our three participants wear the ring on the ring finger, but still use their index finger for pointing. We used the same training and testing procedure as described above.

We found that spatial accuracy was comparable to our previous results (mean error of 8.7mm, SD=8.3mm). However, touch/no-touch classification dropped to 85.0% (SD=9.1%). We hypothesize this is due to multipath issues and also simply a longer signal path to the index finger's tip.

EXAMPLE APPLICATIONS
We built several illustrative applications that highlight SkinTrack's potential to expand the interaction space of wearable devices. To create interactive applications, we combined our sensor band with a LG G smartwatch. Using this platform (Figures 1 and 11-16), we built several applications that demonstrate different interaction modalities enabled by SkinTrack. These include buttons on the skin, scrolling content, directional swiping gestures, and panning of 2D content, among others. We now describe these interactions in greater detail (please also see Video Figure).

Game Controller. SkinTrack mitigates screen occlusion by expanding smartwatch interaction out onto the user's skin. Continuous 2D tracking on the skin affords complex interactions suitable in e.g., gaming applications. For example, a user can play Angry Birds by dragging on the skin. Touching and dragging on the skin (Figure 1A-B) sets the projectile angle and velocity.

Hierarchical Navigation and Continuous Scrolling. SkinTrack also supports discrete directional swiping gestures and 1D continuous, slider-style touch tracking. For example, a user can navigate through a list of applications by swiping up and down (Figure 11A-B). Swiping right selects the current item (e.g., music app as in Figure 11C). The
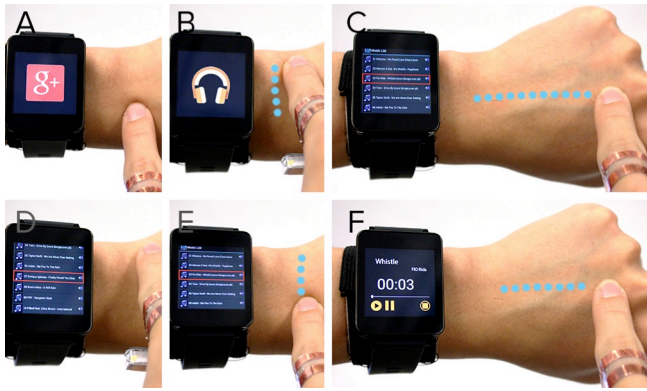
Figure 11. Swiping up or down navigates between apps (A,B). Swiping right launches the selected app (C). Sliding can also be used to continiously scroll a playlist (D,E); swiping right plays the selected song.

skin can then be used as a 1D continuous slider to scroll through a playlist (Figure 11D-E). Finally, swiping right plays the selected song (Figure 11F).

Buttons and Keys. SkinTrack can also detect touches within a discrete 2D space, for example, a number keypad (Figure 12), where the back of the hand can be used to dial a phone number (Figure 12B). Hover tracking is used to provide an on-screen cursor to assist in targeting (Figure 12A,C).

Map Navigation. Interactive functions can be designated to specific regions on the skin. For example, in a map application, the user can zoom in and out by scrolling on the *hand* (right of smartwatch, Figure 13A-B). Likewise, the map can be panned by dragging on the *arm* (left of smartwatch, Figure 13C-D). Tapping the screen brings up additional information on the selected point of interest (Figure 13E).

Drawing. Users' fingers can be used as triggers for specific functions or events. For example, in a drawing application, the index finger and thumb can be used to toggle color selection (Figure 14A,C), while the back of the hand serves as a drawing canvas (Figure 14B,D). The smartwatch screen provides real-time and un-occluded graphics.

Figure 12. The back of the hand can be used as a number keypad. Finger hover location controls an on-screen cursor (A,C) to assist in targetting buttons (B).

Skin App Shortcuts. Synergistic interactions between the touchscreen and skin are also possible. For example, a user can designate spatial shortcuts by "dragging" app icons off of the screen and onto the skin (Figure 15A-D). Apps can then be quickly launched by tapping the corresponding skin location (Figure 15E-F), which launches the appropriate app on the smartwatch.

Global Gestures and Fast Scrolling. Finally, SkinTrack can also offer 2D gestures, which can be used to launch global commands. For example, a user can draw an "N" on their skin to launch a news app (Figure 16A-B). Or draw an "A" to open the address book (Figure 16C-D). While in the address book app, the touch screen can be used for fine-grained scrolling through contacts, while the skin is used for fast alphabetic scrolling (Figure 16E-F).

LIMITATIONS

The most significant obstacle to SkinTrack commercialization is sensing stability across time. Like other bio-sensing systems, we observed slight signal changes over the course of a day, even without removal. The fact is, the human body is in constant motion and skin condition naturally varies (i.e., hydration, sweat etc.). As noted previously, insulating our electrodes with Mylar reduced sensitivity to such skin changes. This might be further dampened with a longer training process and superior materials and ergonomics. Also noted earlier is the accuracy drop following sensor removal. One possible compromise solution is to perform rapid calibration upon replacement (e.g., touching several known points), which tweaks parameters to once again establish accurate tracking.
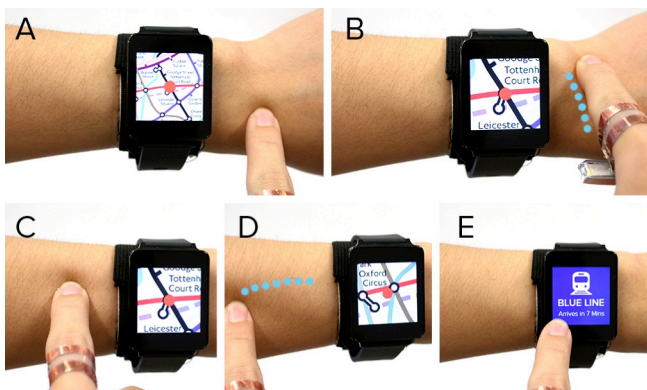

Figure 13. 1D Scrolling on hand zooms map (A,B). 2D Scrolling on the arm controls panning (C,D). Clicking the touchscreen triggers selection (E).
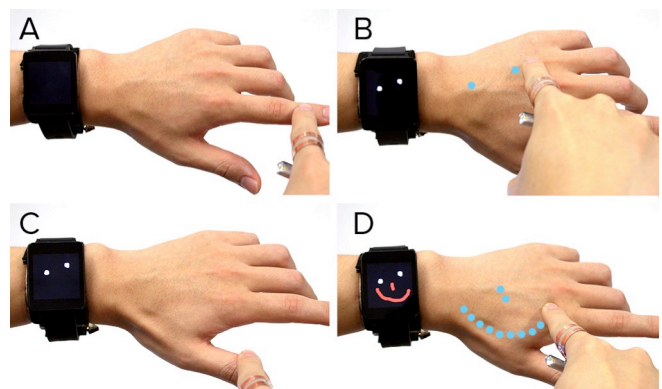

Figure 14. Thumb and index finger toggle color selection (A,C). The back of the hand is used as a drawing canvas (B,D).
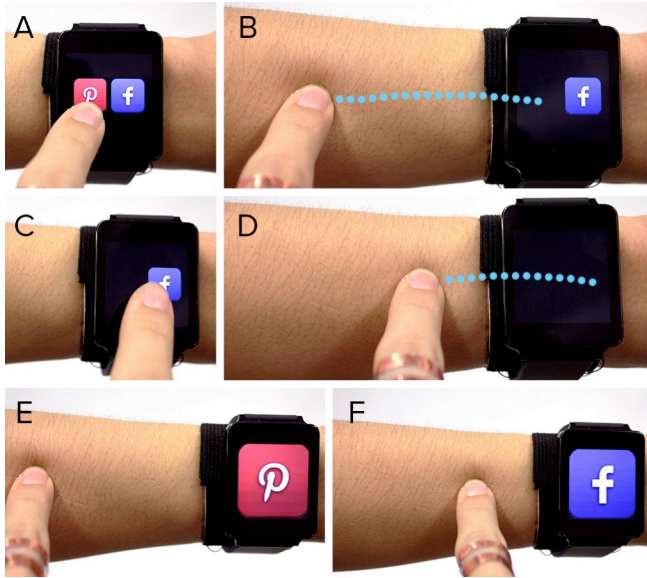
Figure 15. App icons can be dragged from the smartwatch screen onto a skin location (A-D). Afterwards, tapping on the skin location launches the corresponding application (E,F).
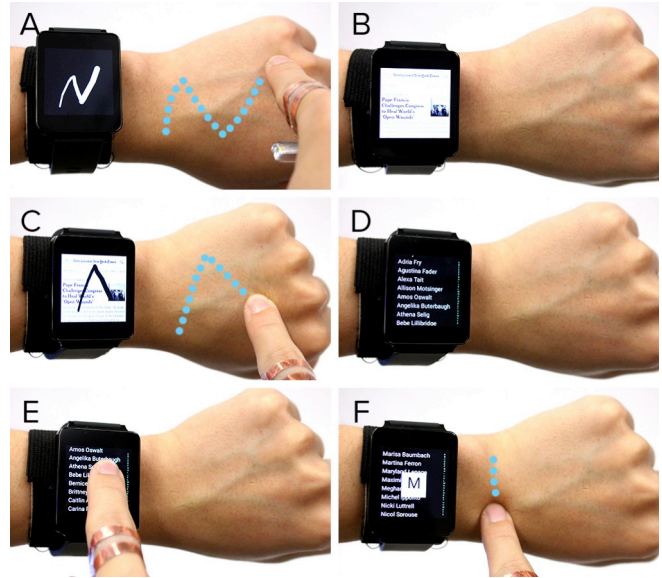

Figure 16. Global gestures can be assigned to applications, such as "N" for news (A,B) or "A" for address book (C,D). Additionally, the touchscreen can be used for fine-grained scrolling (E), while the skin offers a rapid alphabetic scroll (F).

Another issue is powering our signal-emitting ring. Although our circuit design is relatively power efficient, the ring must continuously emit a signal. One solution to reduce power consumption is to adopt advanced filters on the sensor band. This could lower the ring's signal amplitude (saving power) without affecting SNR. Another solution is to dynamically activate signal emission, perhaps in response to a capacitive change or vibro-acoustic event indicative of a finger touch. This could significantly reduce the duty cycle of the signal output (though other processes would have to be running instead).

Finally, we also noticed that the physical contact condition of the finger pressed to the skin can affect the reported position. For example, pressing hard with the finger (i.e., with above average pressure) caused the system to report movement, though the position was actually static. Likewise, changes in finger orientation (e.g., pitch and yaw) also affected position estimation, due to through-air coupling. It is possible that the use of superior filters, different frequencies, or even multiple frequencies could resolve this issue, though more research is required.

DISCUSSION

We found no studies in the literature indicating a link between low-level electric or magnetic fields and disease. In fact, the human body is under low-level electrical excitation by commonplace devices all the time. For instance, touchscreens measure a small amount of current drawn by the finger to detect touch positions. Digital scales that measure BMI use a similar signal for measurement [12,51]. Even under fluorescent light, a small current is induced by electromagnetic noise.

It also does not appear that SkinTrack interferes with other electronic devices. For example, in our example applications (see Video Figure), SkinTrack works together with a conventional touchscreen. This is mainly because they operate at different frequency ranges, and their respective internal filters suppress unwanted signals. However, more expansive investigation is required to ensure sure there is not detrimental interference.

CONCLUSION

In this work, we have described SkinTrack, a novel sensing technique that enables continuous finger tracking on the skins' surface from a sensor-instrumented smartwatch. The user needs only to wear a special ring, which emits an active signal. To characterize our approach, we described a series of evaluations investigating over a dozen different performance metrics relevant to SkinTrack. When trained on a user, our approach can accurately detect touch events at 99% accuracy, and resolve touch locations to within 7.6mm on average. This is approaching touchscreen-like accuracy and can be used to support a wide range of rich interactive functionalities. This work not only sets a new bar for on-skin touch tracking accuracy, but also enables it in a more practical form factor than previous methods.

REFERENCES

1. Daniel Ashbrook, Kent Lyons, and Thad Starner. 2008. An investigation into round touchscreen wristwatch interaction. In *Proceedings of the 10th International Conference on Human Computer Interaction with Mobile Devices and Services* (MobileHCI '08), 311-314. http://dx.doi.org/10.1145/1409240.1409276

2. Daniel Ashbrook, Patrick Baudisch, and Sean White. 2011. Nenya: subtle and eyes-free mobile input with a magnetically-tracked finger ring. In *Proceedings of the SIGCHI Conference on Human Factors in Computing Systems* (CHI '11), 2043-2046. http://dx.doi.org/10.1145/1978942.1979238

3. Patrick Baudisch and Gerry Chu. 2009. Back-of-device interaction allows creating very small touch devices. In *Proceedings of the SIGCHI Conference on Human Factors in Computing Systems* (CHI '09), 1923-1932. http://dx.doi.org/10.1145/1518701.1518995

4. Liwei Chan, Yi-Ling Chen, Chi-Hao Hsieh, Rong-Hao Liang, and Bing-Yu Chen. 2015. CyclopsRing: Enabling Whole-Hand and Context-Aware Interactions Through a Fisheye Ring. In *Proceedings of the 28th Annual ACM Symposium on User Interface Software and Technology* (UIST '15), 549-556. http://dx.doi.org/10.1145/2807442.2807450

5. Xiang Chen, Julia Schwarz, Chris Harrison, Jennifer Mankoff, and Scott E. Hudson. 2014. Air+touch: interweaving touch & in-air gestures. In *Proceedings of the 27th Annual ACM Symposium on User Interface Software and Technology* (UIST '14), 519-525. http://doi.acm.org/10.1145/2642918.2647392

6. Ke-Yu Chen, Kent Lyons, Sean White, and Shwetak Patel. 2013. uTrack: 3D input using two magnetic sensors. In *Proceedings of the 26th Annual ACM Symposium on User Interface Software and Technology* (UIST '13), 237-244. http://dx.doi.org/10.1145/2501988.2502035

7. Gabe Cohn, Daniel Morris, Shwetak Patel, and Desney Tan. 2012. Humantenna: Using the Body as an Antenna for Real-Time Whole-Body Interaction. *Proceedings of the 2012 ACM Annual Conference on Human Factors in Computing Systems* (CHI '12), 1901-1910. http://doi.org/10.1145/2207676.2208330

8. Gabe Cohn, Daniel Morris, Shwetak N. Patel, and Desney S. Tan. 2011. Your noise is my command: sensing gestures using the body as an antenna. In *Proceedings of the SIGCHI Conference on Human Factors in Computing Systems* (CHI '11), 791-800. http://dx.doi.org/10.1145/1978942.1979058

9. Analog Devices, Inc. AD8302 RF/IF Gain and Phase Detector. Revision A. Published in 2002. http://www.analog.com/media/cn/technical-documentation/data-sheets/AD8302.pdf Last Retrieved: January 6, 2016

10. Niloofar Dezfuli, Mohammadreza Khalilbeigi, Jochen Huber, Florian Müller, and Max Mühlhäuser. 2012. PalmRC: imaginary palm-based remote control for eyes-free television interaction. In *Proceedings of the 10th European Conference on Interactive TV and Video* (EuroiTV '12), 27-34. http://dx.doi.org/10.1145/2325616.2325623

11. Paul Dietz and Darren Leigh. 2001. DiamondTouch: a multi-user touch technology. In *Proceedings of the 14th Annual ACM Symposium on User Interface Software and Technology* (UIST '01), 219-226. http://dx.doi.org/10.1145/502348.502389

12. Fitbit, Inc. http://www.fitbit.com/aria

13. Katsuyuki Fuji, Koichi Ito, and Shigeru Tajima. 2003. A study on the receiving signal level in relation with the location of electrodes for wearable devices using human body as a transmission channel. *IEEE Antennas and Propagation Society International Symposium. Digest. Held in conjunction with: USNC/CNC/URSI North American Radio Sci. Meeting (Cat. No.03CH37450)* 3: 1071–1074. http://doi.org/10.1109/APS.2003.1220096

14. T. G. Zimmerman. 1996. Personal area networks: near-field intrabody communication. *IBM Syst. J.* 35, 3-4 (September 1996), 609-617. http://dx.doi.org/10.1147/sj.353.0609

15. C Gabriel, S Gabriel, and E Corthout. 1996. The dielectric properties of biological tissues: I. Literature survey. *Physics in medicine and biology* 41, 11: 2231–49. http://doi.org/10.1088/0031-9155/41/11/001

16. Keisuke Hachisuka, Azusa Nakata, Teruhito Takeda, Yusuke Terauchi, Kenji Shiba, Ken Sasaki, Hiroshi Hosaka, and Kiyoshi Itao. 2003. Development and performance analysis of an intra-body communication device. *12th International Conference on Solid-State Sensors, Actuators and Microsystems. Digest of Technical Papers* (TRANSDUCERS '03) (Cat. No.03TH8664) 2: 1722–1725. http://doi.org/10.1109/SENSOR.2003.1217117

17. Mark Hall, Eibe Frank, Geoffrey Holmes, Bernhard Pfahringer, Peter Reutemann, and Ian H. Witten. 2009. The WEKA data mining software: an update. *SIGKDD Explor. Newsl.* 11, 1 (November 2009), 10-18. http://dx.doi.org/10.1145/1656274.1656278

18. Chris Harrison and Scott E. Hudson. 2009. Abracadabra: wireless, high-precision, and unpowered finger input for very small mobile devices. In *Proceedings of the 22nd Annual ACM Symposium on User Interface Software and Technology* (UIST '09), 121-124. http://dx.doi.org/10.1145/1622176.1622199

19. Chris Harrison, Desney Tan, and Dan Morris. 2010. Skinput: appropriating the body as an input surface. In *Proceedings of the SIGCHI Conference on Human Factors in Computing Systems* (CHI '10), 453-462. http://dx.doi.org/10.1145/1753326.1753394

20. Chris Harrison, Hrvoje Benko, and Andrew D. Wilson. 2011. OmniTouch: wearable multitouch interaction everywhere. In *Proceedings of the 24th Annual ACM Symposium on User Interface Software and Technology* (UIST '11), 441-450. http://dx.doi.org/10.1145/2047196.2047255

21. Chris Harrison, Munehiko Sato, and Ivan Poupyrev. 2012. Capacitive fingerprinting: exploring user differentiation by sensing electrical properties of the human body. In *Proceedings of the 25th Annual ACM Symposium on User Interface Software and Technology* (UIST '12), 537-544. http://dx.doi.org/10.1145/2380116.2380183

22. Christian Holz and Patrick Baudisch. 2010. The generalized perceived input point model and how to double touch accuracy by extracting fingerprints. In *Proceedings of the SIGCHI Conference on Human Factors in Computing Systems* (CHI '10), 581-590. http://dx.doi.org/10.1145/1753326.1753413

23. Christian Holz, Tovi Grossman, George Fitzmaurice, and Anne Agur. 2012. Implanted user interfaces. In *Proceedings of the SIGCHI Conference on Human Factors in Computing Systems* (CHI '12), 503-512. http://dx.doi.org/10.1145/2207676.2207745

24. Christian Holz and Marius Knaust. 2015. Biometric Touch Sensing: Seamlessly Augmenting Each Touch with Continuous Authentication. In *Proceedings of the 28th Annual ACM Symposium on User Interface Software and Technology* (UIST '15), 303-312. http://dx.doi.org/10.1145/2807442.2807458

25. Sophocles J. Orfanidis. 2008. Electromagnetic Waves and Antennas: Waveguides. *Rutgers University.*

26. Rebecca K. Kramer, Carmel Majidi, Robert J. Wood. 2011. Wearable tactile keypad with stretchable artificial skin. In *Proceedings of the IEEE International Conference on Robotics and Automation (ICRA '11)*, 1103-1107. http://doi.org/10.1109/ICRA.2011.5980082

27. Wolf Kienzle and Ken Hinckley. 2014. LightRing: always-available 2D input on any surface. In *Proceedings of the 27th Annual ACM Symposium on User Interface Software and Technology* (UIST '14), 157-160. http://dx.doi.org/10.1145/2642918.2647376

28. Dae-Hyeong Kim et al. Epidermal Electronics. Science 333, 6044 (2011), 838-843.

29. Jungsoo Kim, Jiasheng He, Kent Lyons, and Thad Starner. 2007. The Gesture Watch: A Wireless Contact-free Gesture based Wrist Interface. In *Proceedings of the 11th IEEE International Symposium on Wearable Computers* (ISWC '07) Figure 1: 1–8. http://doi.org/10.1109/ISWC.2007.4373770

30. Sven Kratz and Michael Rohs. 2009. Hoverflow: exploring around-device interaction with IR distance sensors. In *Proceedings of the 11th International Conference on Human-Computer Interaction with Mobile Devices and Services* (MobileHCI '09), Article 42 , 4 pages. http://dx.doi.org/10.1145/1613858.1613912

31. Gierad Laput, Robert Xiao, Xiang 'Anthony' Chen, Scott E. Hudson, and Chris Harrison. 2014. Skin buttons: cheap, small, low-powered and clickable fixed-icon laser projectors. In *Proceedings of the 27th Annual ACM Symposium on User Interface Software and Technology* (UIST '14), *389-394.* http://doi.acm.org/10.1145/2642918.2647356

32. Gierad Laput, Chouchang Yang, Robert Xiao, Alanson Sample, and Chris Harrison. 2015. EM-Sense: Touch Recognition of Uninstrumented, Electrical and Electromechanical Objects. In *Proceedings of the 28th Annual ACM Symposium on User Interface Software and Technology* (UIST '15), 157-166. http://dx.doi.org/10.1145/2807442.2807481

33. Rong-Hao Liang, Shu-Yang Lin, Chao-Huai Su, Kai-Yin Cheng, Bing-Yu Chen, and De-Nian Yang. 2011. SonarWatch: appropriating the forearm as a slider bar. In *SIGGRAPH Asia 2011 Emerging Technologies* (SA '11), Article 5, 1 pages. http://dx.doi.org/10.1145/2073370.2073374

34. Chia-Hsien Lin and Koichi Ito. 2014. A Compact Dual-Mode Wearable Antenna for Body-Centric Wireless Communications. In *Electronics 2014*, 3, 398-408.

35. Denys J. C. Matthies, Simon T. Perrault, Bodo Urban, and Shengdong Zhao. 2015. Botential: Localizing On-Body Gestures by Measuring Electrical Signatures on the Human Skin. In *Proceedings of the 17th International Conference on Human-Computer Interaction with Mobile Devices and Services* (MobileHCI '15), 207-216. http://dx.doi.org/10.1145/2785830.2785859

36. Adiyan Mujibiya, Xiang Cao, Desney S. Tan, Dan Morris, Shwetak N. Patel, and Jun Rekimoto. 2013. The sound of touch: on-body touch and gesture sensing based on transdermal ultrasound propagation. In *Proceedings of the 2013 ACM International Conference on Interactive Tabletops and Surfaces* (ITS '13), 189-198. http://dx.doi.org/10.1145/2512349.2512821

37. Kei Nakatsuma, Hiroyuki Shinoda, Yasutoshi Makino, Katsunari Sato, and Takashi Maeno. 2011. Touch interface on back of the hand. In *ACM SIGGRAPH 2011 Posters* (SIGGRAPH '11), Article 39 , 1 pages. http://dx.doi.org/10.1145/2037715.2037760

38. Tao Ni and Patrick Baudisch. 2009. Disappearing mobile devices. In *Proceedings of the 22nd Annual ACM Symposium on User Interface Software and Technology* (UIST '09), 101-110. http://dx.doi.org/10.1145/1622176.1622197

39. Shahriar Nirjon, Jeremy Gummeson, Dan Gelb, and Kyu-Han Kim. 2015. TypingRing: A Wearable Ring Platform for Text Input. In *Proceedings of the 13th Annual International Conference on Mobile Systems, Applications and Services* (MobiSys '15), 227-239. http://dx.doi.org/10.1145/2742647.2742665

40. Masa Ogata, Yuta Sugiura, Yasutoshi Makino, Masahiko Inami, and Michita Imai. 2013. SenSkin: adapting skin as a soft interface. In *Proceedings of the 26th Annual ACM Symposium on User Interface Software and Technology* (UIST '13), 539-544. http://dx.doi.org/10.1145/2501988.2502039

41. Manuel Prätorius, Aaron Scherzinger, and Klaus Hinrichs. 2015. SkInteract: An On-body Interaction System Based on Skin-Texture Recognition. Human-Computer Interaction (INTERACT '15), 425-432. http://dx.doi.org/10.1007/978-3-319-22723-8_34

42. Shanaka Ransiri, Roshan Lalintha Peiris, Kian Peen Yeo, and Suranga Nanayakkara. 2013. SmartFinger: connecting devices, objects and people seamlessly. *In Proceedings of the 25th Australian Computer-Human Interaction Conference: Augmentation, Application, Innovation, Collaboration* (OzCHI '13), 359-362. http://dx.doi.org/10.1145/2541016.2541064

43. E. Rehmi Post and Margaret Orth. 1997. Smart Fabric, or "Wearable Clothing". In *Proceedings of the 1st IEEE International Symposium on Wearable Computers* (ISWC '97), 167-168. http://doi.org/10.1109/ISWC.1997.629937

44. J. Rekimoto. 2001. GestureWrist and GesturePad: unobtrusive wearable interaction devices. In *Proceedings Fifth International Symposium on Wearable Computers.* (ISWC '01), 21-27. http://doi.org/10.1109/ISWC.2001.962092

45. Thijs Roumen, Simon T. Perrault, and Shengdong Zhao. 2015. NotiRing: A Comparative Study of Notification Channels for Wearable Interactive Rings. In *Proceedings of the 33rd Annual ACM Conference on Human Factors in Computing Systems* (CHI '15), 2497-2500. http://dx.doi.org/10.1145/2702123.2702350

46. Peter S. Hall and Yang Hao. 2012. Antennas and Propagation for Body-Centric Wireless Communications. *Artech House; 2nd edition.*

47. Scott Saponas, Desney S. Tan, Dan Morris, and Ravin Balakrishnan. 2008. Demonstrating the feasibility of using forearm electromyography for muscle-computer interfaces. In *Proceedings of the SIGCHI Conference on Human Factors in Computing Systems* (CHI '08), 515-524. http://doi.acm.org/10.1145/1357054.1357138

48. Scott Saponas, Desney S. Tan, Dan Morris, Ravin Balakrishnan, Jim Turner, and James A. Landay. 2009. Enabling always-available input with muscle-computer interfaces. In *Proceedings of the 22nd Annual ACM Symposium on User Interface Software and Technology* (UIST '09), 167-176. http://doi.acm.org/10.1145/1622176.1622208

49. Munehiko Sato, Ivan Poupyrev, and Chris Harrison. 2012. Touché: enhancing touch interaction on humans, screens, liquids, and everyday objects. In *Proceedings of the SIGCHI Conference on Human Factors in Computing Systems* (CHI '12), 483-492. http://dx.doi.org/10.1145/2207676.2207743

50. Tsuyoshi Sekitani, Martin Kaltenbrunner, Tomoyuki Yokota, and Takao Someya. 2014. Imperceptible Electronic Skin. SID Information Display 30, 1, 20-25.

51. Skulput, Inc. http://www.skulpt.me

52. Simon T. Perrault, Eric Lecolinet, James Eagan, and Yves Guiard. 2013. Watchit: simple gestures and eyes-free interaction for wristwatches and bracelets. In *Proceedings of the SIGCHI Conference on Human Factors in Computing Systems* (CHI '13), 1451-1460. http://dx.doi.org/10.1145/2470654.2466192

53. Martin Weigel, Tong Lu, Gilles Bailly, Antti Oulasvirta, Carmel Majidi, and Jürgen Steimle. 2015. iSkin: Flexible, Stretchable and Visually Customizable On-Body Touch Sensors for Mobile Computing. In *Proceedings of the 33rd Annual ACM Conference on Human Factors in Computing Systems* (CHI '15), 2991-3000. http://dx.doi.org/10.1145/2702123.2702391

54. Mathias Wilhelm, Daniel Krakowczyk, Frank Trollmann, and Sahin Albayrak. 2015. eRing: multiple finger gesture recognition with one ring using an electric field. In *Proceedings of the 2nd international Workshop on Sensor-based Activity Recognition and Interaction* (WOAR '15), Article 7 , 6 pages. http://dx.doi.org/10.1145/2790044.2790047

55. Katrin Wolf and Jonas Willaredt. 2015. PickRing: seamless interaction through pick-up detection. In *Proceedings of the 6th Augmented Human International Conference* (AH '15), 13-20. http://dx.doi.org/10.1145/2735711.2735792

56. Robert Xiao, Gierad Laput, and Chris Harrison. 2014. Expanding the input expressivity of smartwatches with mechanical pan, twist, tilt and click. In *Proceedings of the SIGCHI Conference on Human Factors in Computing Systems* (CHI '14), 193-196. http://dx.doi.org/10.1145/2556288.2557017

57. Xing-Dong Yang, Tovi Grossman, Daniel Wigdor, and George Fitzmaurice. 2012. Magic finger: always-available input through finger instrumentation. In *Proceedings of the 25th Annual ACM Symposium on User Interface Software and Technology* (UIST '12), 147-156. http://dx.doi.org/10.1145/2380116.2380137

58. Yang Zhang and Chris Harrison. 2015. Tomo: Wearable, Low-Cost Electrical Impedance Tomography for Hand Gesture Recognition. In *Proceedings of the 28th Annual ACM Symposium on User Interface Software and Technology* (UIST '15), 167-173. http://dx.doi.org/10.1145/2807442.2807480